Asymmetric Magnetic Nanosnowman Loaded with AgPd Nanocage Toward NIR-enhanced Catalytic Activity

Jie Jin[a,*], Haoran Li[a], Hongfa Wang[b], Qunling Fang[c,*], Yunqi Xu[b], Weili Kong[a], Xia Chen[a], Ken Cham-Fai Leung[d], Hailong Wang[b,*], Shouhu Xuan[b]

a School of Materials and Chemical Engineering, Anhui Jianzhu University, Hefei, 230601, PR China

b CAS Key Laboratory of Mechanical Behavior and Design of Materials, Department of Modern Mechanics, University of Science and Technology of China, Hefei, 230026, PR China

c School of Food and Biological Engineering, Hefei University of Technology, Hefei, 230009, PR China

d State Key Laboratory of Environmental and Biological Analysis, Department of Chemistry, Hong Kong Baptist University, Kowloon, Hong Kong Special Administrative Region of China

*Corresponding author:

Asso. Prof. Jie Jin

E-mail: jinjie@ahjzu.edu.cn

Asso. Prof. Qunling Fang

E-mail: fql.good@hfut.edu.cn

Prof. Hailong Wang

E-mail: hailwang@ustc.edu.cn

Experimental section

Materials

Iron (III) chloride hexahydrate ($FeCl_3 \cdot 6H_2O$), Poly(acrylic acid) (PAA, ~2000), Sodium citrate ($C_6H_5Na_3O_7 \cdot 2H_2O$), Ethanol (EtOH), Urea (H_2NCONH_2), Silver nitrate ($AgNO_3$), Ammonium hydroxide ($NH_3 \cdot H_2O$), Palladium (II) chloride ($PdCl_2$), Sodium borohydride ($NaBH_4$), 3-Hydroxytyrosine hydrochloride (DA-HCl), Trihydroxymethyl aminomethane (Tris-HCl), Glacial acetic acid ($C_2H_4O_2$) 4-nitrophenol ($C_6H_5NO_3$), Methylene Blue trihydrate ($C_{16}H_{18}ClN_3S \cdot 3H_2O$), Methyl orange ($CHN_3SO_3Na$) and N,N-Dimethylformamide (DMF, C_3H_7NO) were purchased from Sinopharm Chemical Reagent Co., Ltd. Ethylene glycol (EG, $(CH_2OH)_2$), Polyvinylpyrrolidone (PVP, $(C_6H_9NO)_n$), Iodobenzene (C_6H_5I), 4-Iodotoluene (C_7H_7I), 4-Iodophenetole (C_8H_9IO), 4-Iodoanisole ($IC_6H_4OCH_3$), Bromobenzene (C_6H_5Br), Chlorobenzene (C_6H_5Cl), Methyl acrylate ($C_4H_6O_2$), Triethylamine ($C_6H_{15}N$) and Dichloromethane (CH_2Cl_2) were purchased from Aladdin Chemical Co., Ltd, China. Petroleum ether (PE, $C_5HC_6HC_7H$) and Ethylacetate (EA, $C_4H_8O_2$) were purchased from Macklin Biochemical Technology Co., Ltd. All reagents were used as received without further purification and ultrapure water was used in all experiments.

Synthesis of Fe_3O_4@Ag/PDA nanospheres: First, 15 mg Fe_3O_4 nanospheres were dispersed in 50 mL of ethanol using ultrasonication, followed by the addition of PVP (0.1 g) and further ultrasonication for 1 h. Subsequently, $Ag(NH_3)_2OH$ (0.5 mL, 8.8×10^{-5} M) was introduced under magnetic stirring. After 14 h, the reaction system was transferred to ultrasound at 35 °C. Following a 30 min interval, $NaBH_4$ (10 mg) was added. 30 min later, the Tris-HCl buffer (25 mL, pH=8.5) mixed with dopamine (25 mg) was poured into the conical flask. After 4 h, the products were collected with a magnet and washed alternately with deionized water and ethanol. Finally, the product was obtained by vacuum drying.

Synthesis of Fe_3O_4@Pd/PDA nanospheres: First, 15 mg Fe_3O_4 nanospheres were dispersed in 50 mL of ethanol using ultrasonication, followed by the addition of PVP (0.1 g) and further ultrasonication for 1 h. Subsequently, the mixture was stirred magnetically for 14 h. Then, the reaction system was transferred to ultrasonic waves

at 35 °C. Following a 30 min interval, $NaBH_4$ (10 mg) and H_2PdCl_4 (0.01 M, 4.4 mL) were added. 30 min later, the Tris-HCl buffer (25 mL, pH=8.5) mixed with dopamine (25 mg) was poured into the conical flask. After 4 h, the products were collected with a magnet and washed alternately with deionized water and ethanol. Finally, the product was obtained by vacuum drying.

Synthesis of h-Fe_3O_4@AgPd/PDA nanospheres, MXene@AgPd/PDA nanosheets, α-Fe_2O_3@AgPd@PDA nanospindles, and SiO_2@AgPd/PDA nanospheres: Firstly, h-Fe_3O_4 nanospheres, MXene nanosheets, α-Fe_2O_3 nanospindles, SiO_2 nanospheres were synthesized by literatures[1-4]. The subsequent synthesis methods were consistent with those of Fe_3O_4@AgPd/PDA nanosnowman.

DFT calculation details

The density functional theory (DFT) calculation was carried out using Vienna Ab initio Simulation Package (VASP). The exchange–correlation energy functional was described by Perdew-Burke-Ernzerhof generalized gradient approximation (GGA-PBE). The projector augmented wave (PAW) pseudopotentials were used to describe the core electrons interaction. The Brillouin zone integration was performed using a grid of 4×4×1 Gamma center scheme, which was corresponded to a density of 0.04 2π/Å. The plane wave energy cutoff was set to 420 eV, while the vacuum region was set to 15 Å. The energy convergence threshold was set to 10^{-6} eV and the force threshold was set to 0.01 eV/Å. The heterostructures were constituted of Fe_3O_4 (110) and AgPd (111), comprising 48 Fe atoms, 64 O atoms, 12 Ag atoms, and 12 Pd atoms.

The charge density difference was calculated by the formula,

$$\Delta\rho = \rho(AgPd@Fe_3O_4) - \rho(AgPd) - \rho(Fe_3O_4) \qquad (3)$$

Where the $\rho(AgPd@Fe_3O_4)$, $\rho(AgPd)$, $\rho(Fe_3O_4)$ were the charge density of AgPd@Fe_3O_4, AgPd, and Fe_3O_4, respectively.

Characterization

Field emission transmission electron microscopy (FE-TEM, JEM-2100F) was used to observe the morphology and nanostructure of the samples. Field emission scanning electron microscopy (FE-SEM) images were obtained on a Regulus 8230 HR-FESEM.

The crystal structure of the samples was determined by X-ray diffraction (XRD, SmartLab). The surface elemental composition, chemical states, and electronic structure of the material were determined by an X-ray photoelectron spectrometer (XPS, ESCALAB250Xi). The functional groups of all samples in the range of 4000-500 cm^{-1} wave number were analyzed by FT-IR (Nicolet 6700). An inductively coupled plasma-mass spectrometer (ICP-AES, iCAP 7400) was used to analyze the metal content in the products. An UV spectrophotometer (UV-1800, Shimadzu) was used to determine the absorbance of the substances during the catalytic process. A Gas chromatography-Fourier transform electrostatic field orbital trap ultra-high resolution mass spectrometer (GC-MS, Q Exactive GC) was used to separate and identify the complex components. A nuclear magnetic resonance spectrometer (AV-III 400 MHz NMR) was used to provide information about the chemical environment and bonds of atoms in a compound molecule.
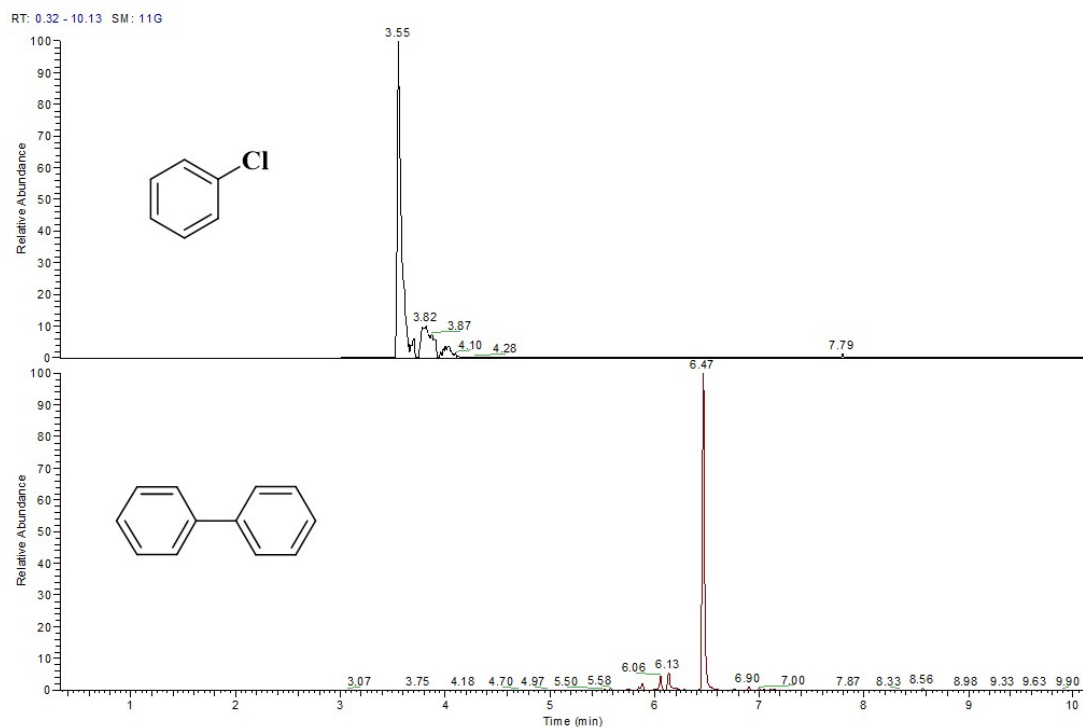
Supplementary Figures
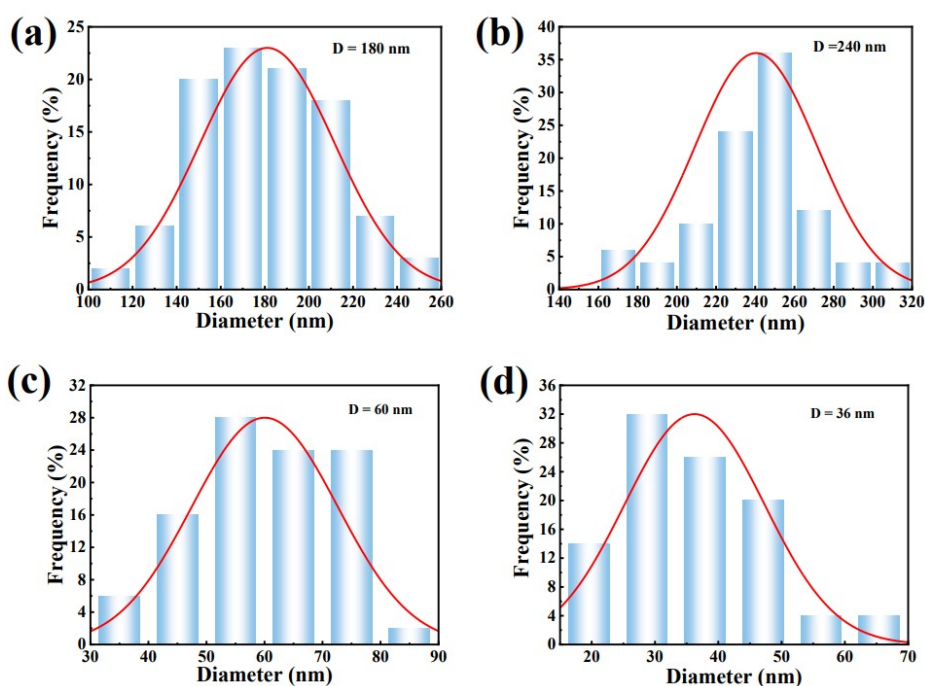
Fig. S1 Size distribution histogram of Fe_3O_4 (a), the "body" of Fe_3O_4@AgPd/PDA nanosnowman (b), the outer diameter of AgPd nanocage (c), and the inner diameter of AgPd nanocage (d).
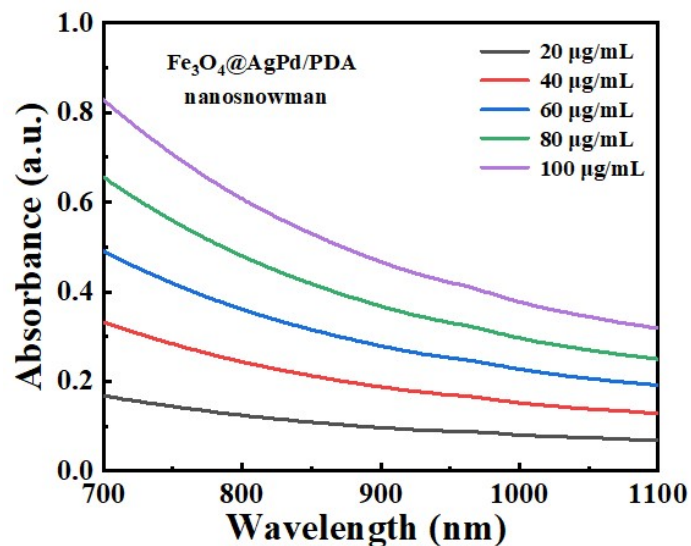
Fig. S2 Near-infrared absorption spectra of the Fe$_3$O$_4$@AgPd/PDA nanosnowman.

**Fig. S3** GC-MS spectra of the products obtained using Fe$_3$O$_4$@AgPd/PDA nanosnowman as a catalyst and chlorobenzene and methyl acrylate as a reaction substrate.
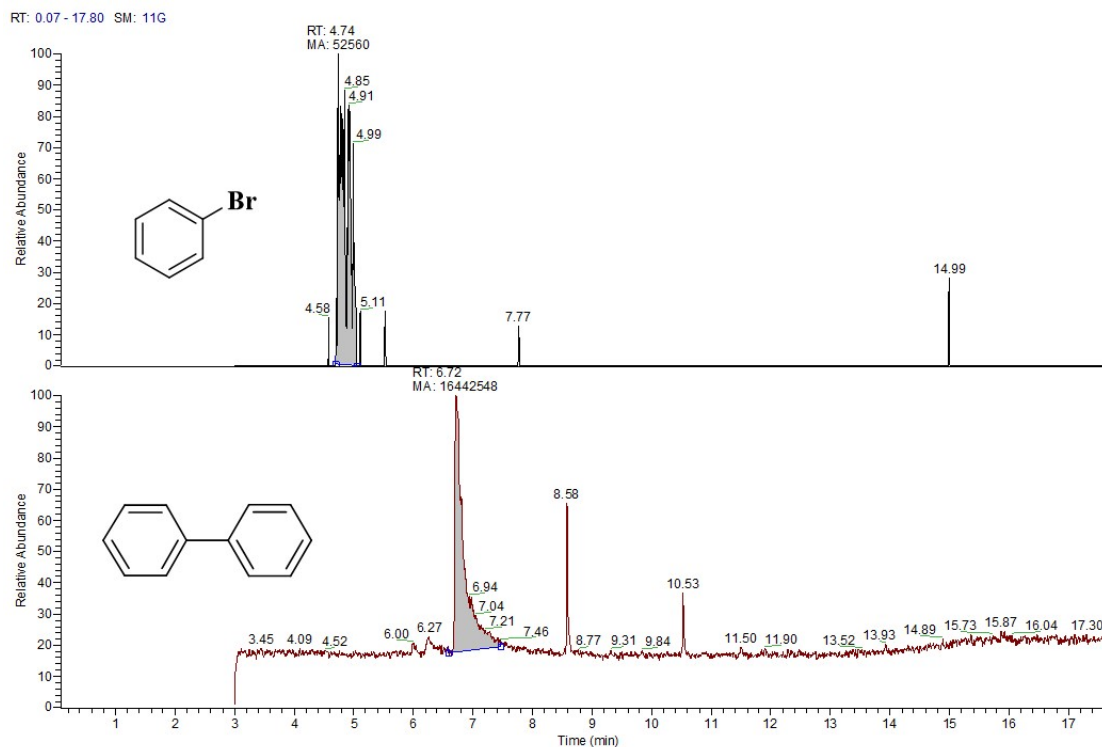
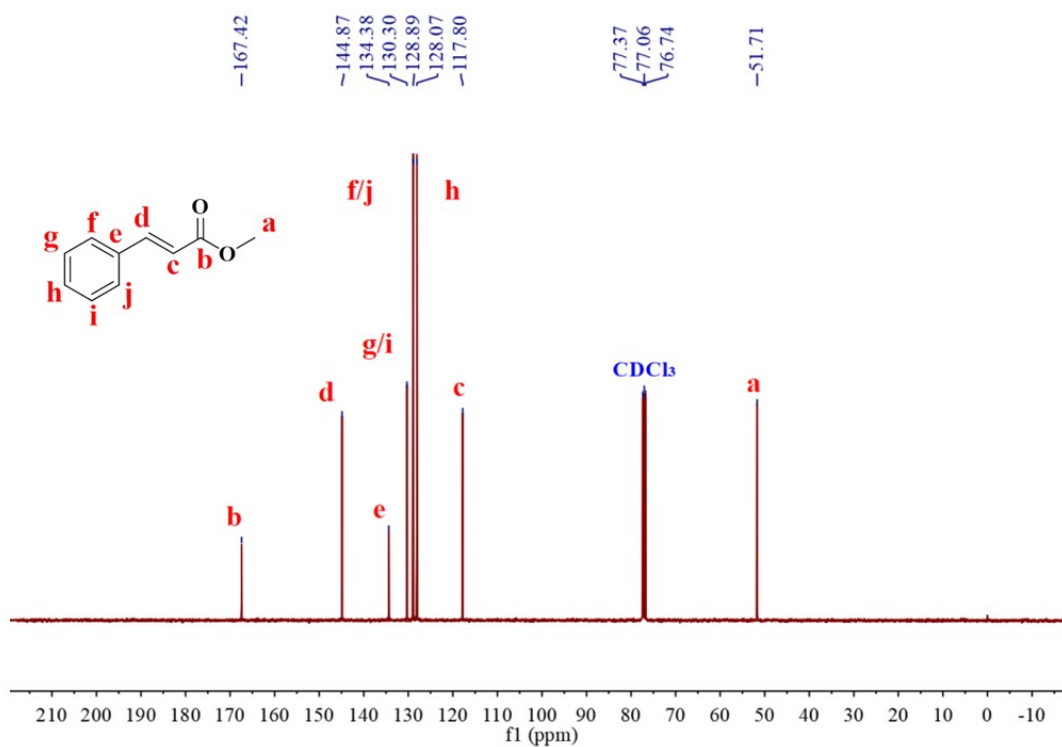**Fig. S4** GC-MS spectra of the products obtained using Fe₃O₄@AgPd/PDA nanosnowman as a catalyst and bromobenzene and methyl acrylate as a reaction substrate.
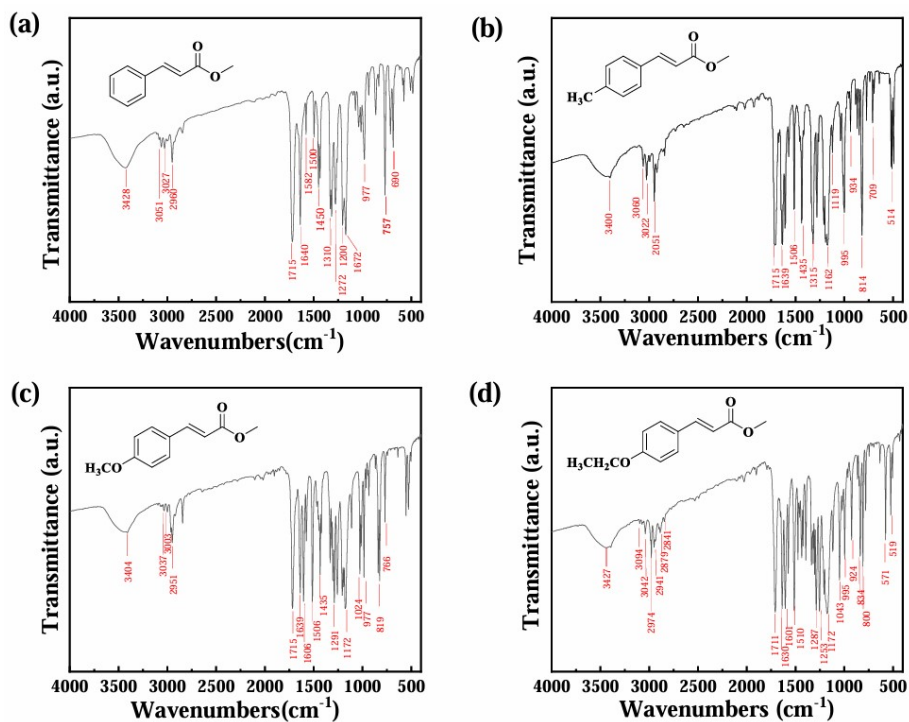
Fig. S5 FTIR spectra of methyl cinnamate, methyl 4-methylcinnamate, methyl (*E*)-p-methoxycinnamate, and methyl 4-ethoxy cinnamate.
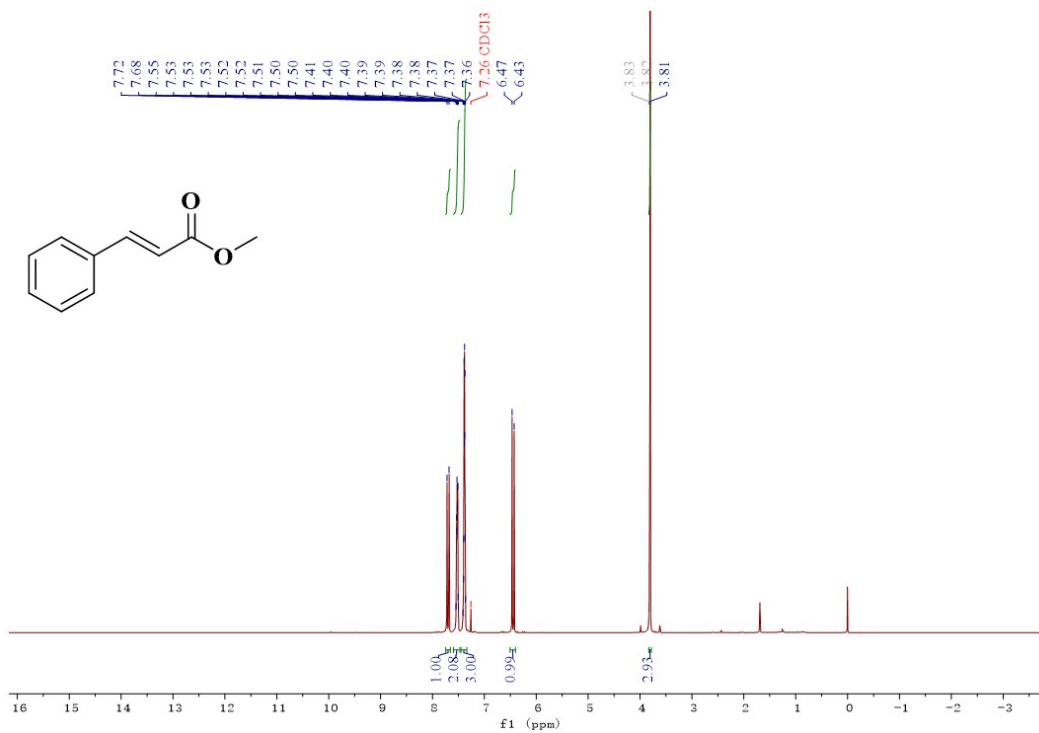
Fig. S6 ^{1}H NMR spectra of methyl cinnamate.

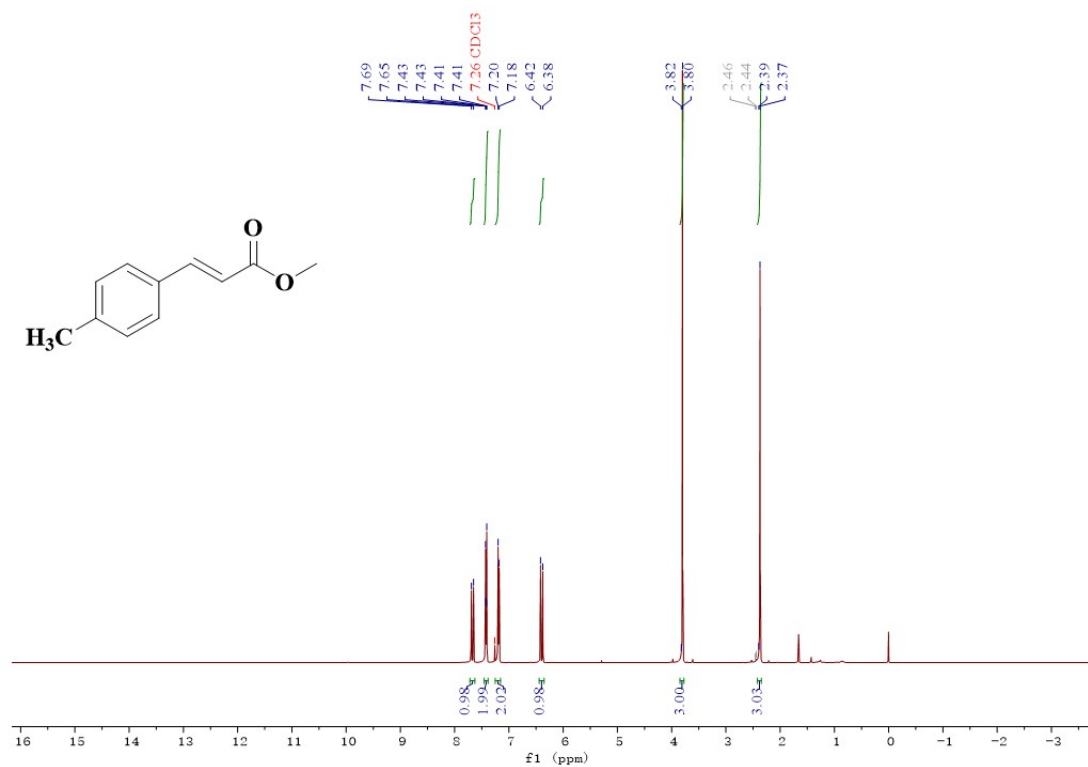**Fig. S7** ^{13}C NMR spectra of methyl cinnamate.

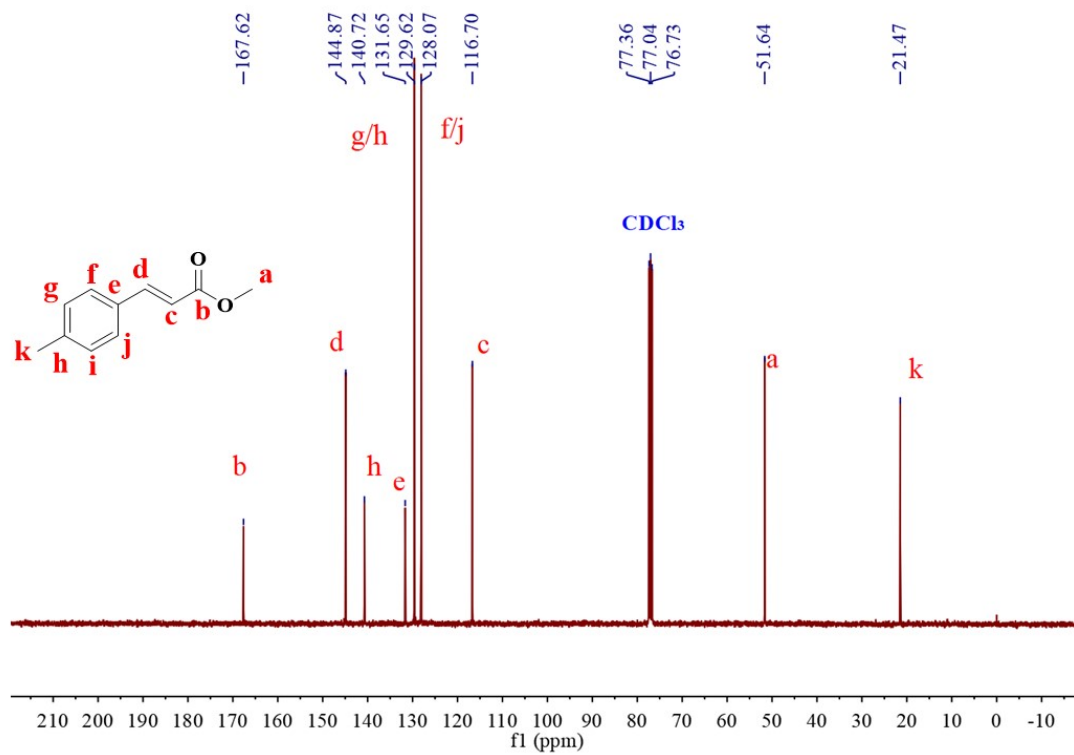**Fig. S8** ^{1}H NMR spectra of methyl 4-methylcinnamate.

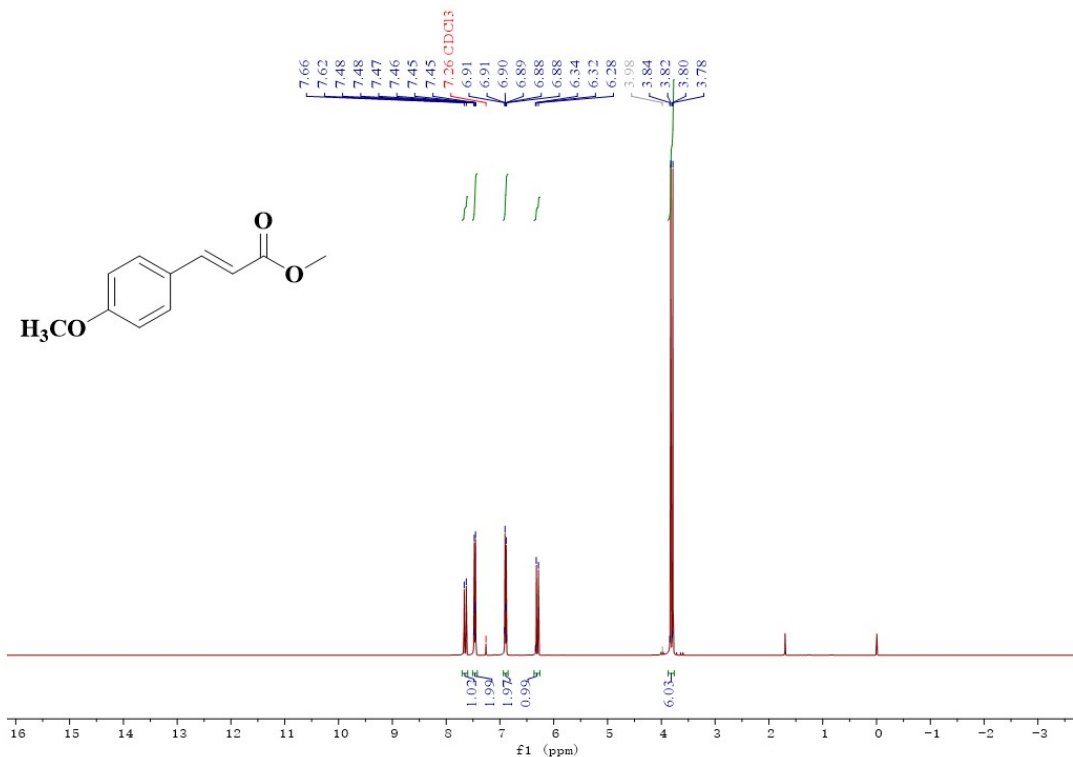**Fig. S9** ^{13}C NMR spectra of methyl 4-methylcinnamate.

Fig. S10 ^{1}H NMR spectra of methyl (*E*)-p-methoxycinnamate.
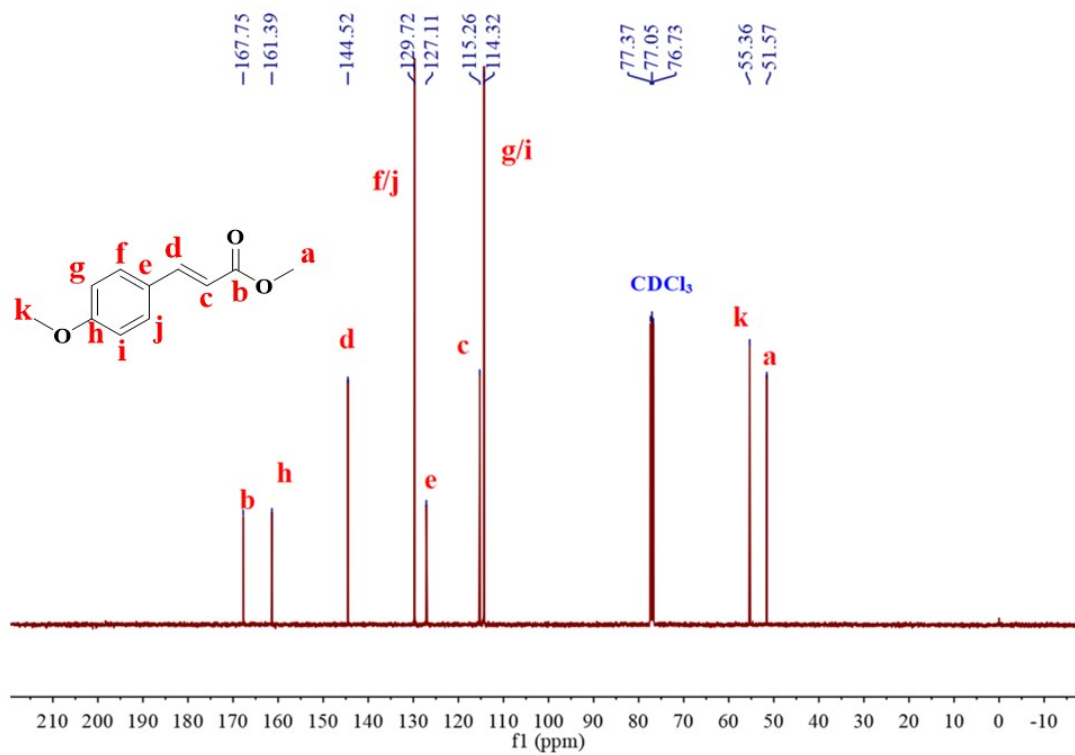

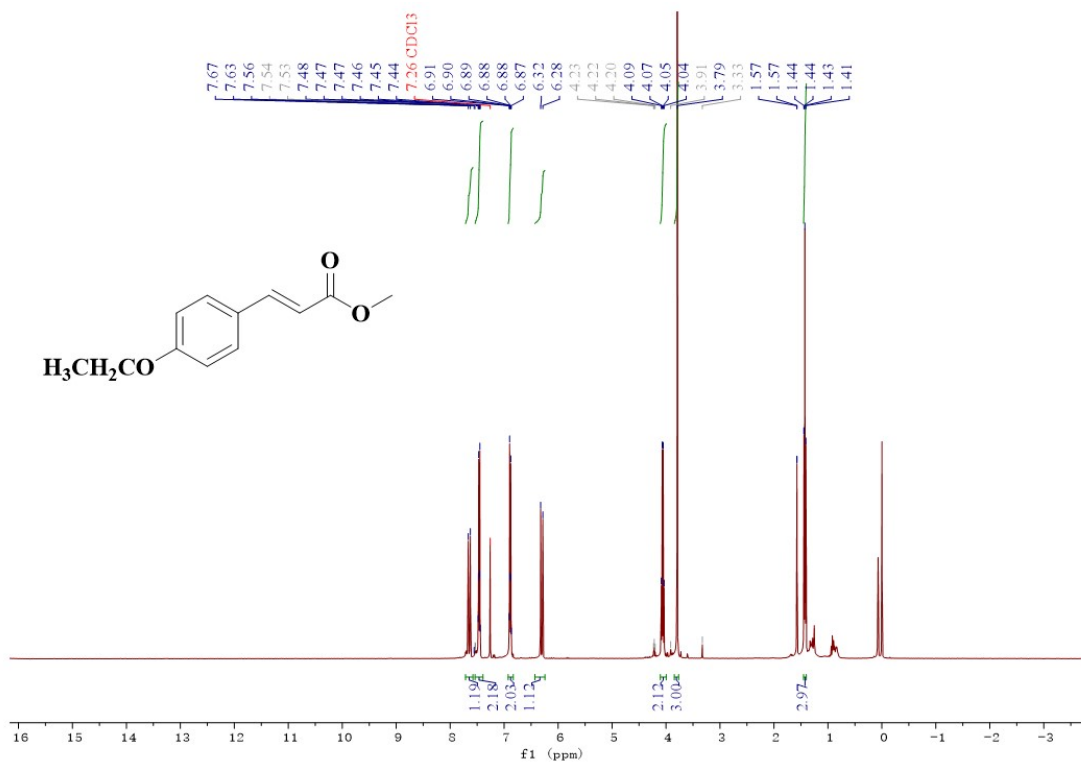**Fig. S11** ^{13}C NMR spectra of methyl (*E*)-p-methoxycinnamate.

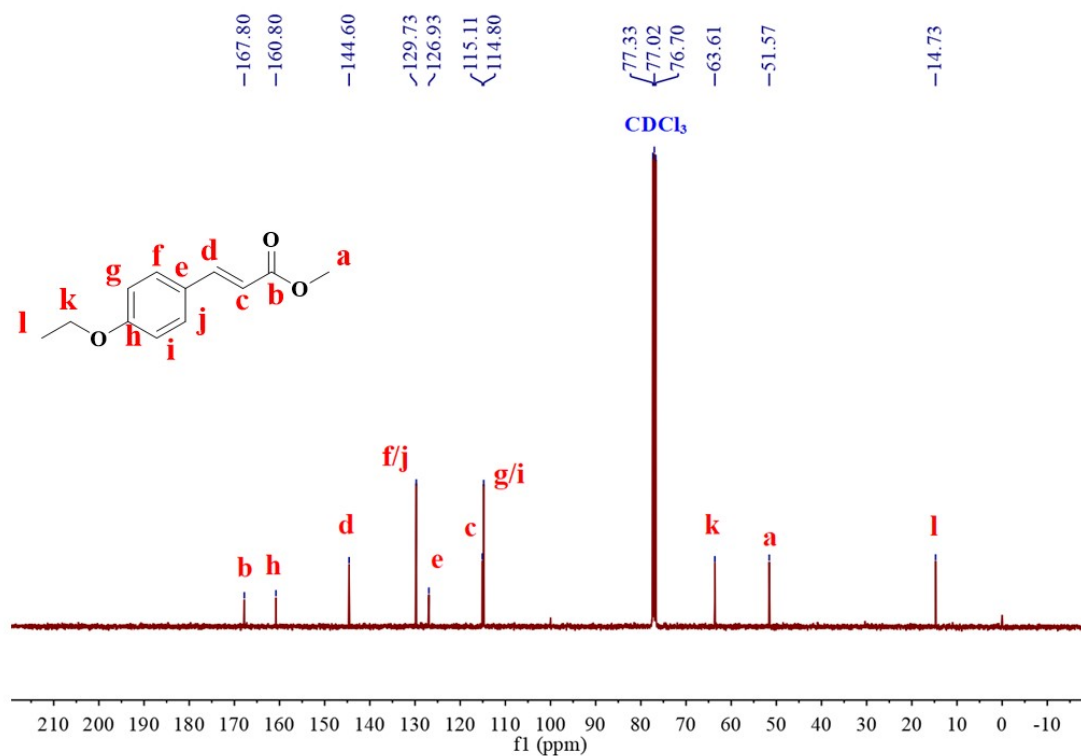**Fig. S12** ^{1}H NMR spectra of methyl 4-ethoxy cinnamate.

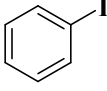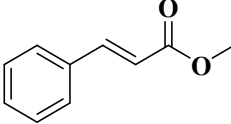**Fig. S13** ^{13}C NMR spectra of methyl 4-ethoxy cinnamate.
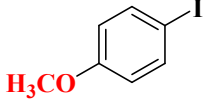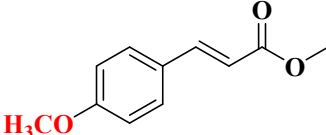
Supporting Tables
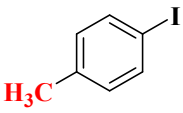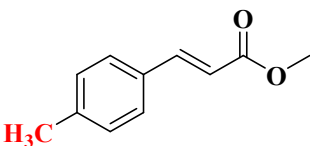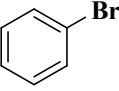
Table. S1 The weight percentage of Ag and Pd elements in samples was determined by ICP-AES.

samples / elements	$Fe_3O_4@Ag/PDA$	$Fe_3O_4@Pd/PDA$	$Fe_3O_4@AgPd/PDA$ nanospheres	$Fe_3O_4@AgPd/PDA$ nanosnowman
Ag	12.2 wt%		6.46 wt%	11.10 wt%
Pd		3.0 wt%	4.59 wt%	6.89 wt%

Table. S2 Comparison of the catalytic capacities of various catalysts reported in the literature for the reduction of 4-NP, MO, and MB by $NaBH_4$.

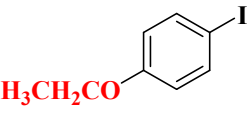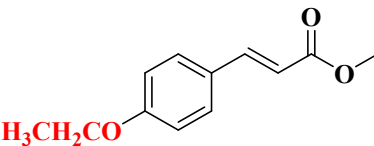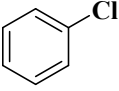| Organic pollutants	Catalysts	k_n (min^{-1} mg^{-1})	References
4-NP	kaolin-PDA-PdAg	0.3456	[5]
	UiO-66/btb/Pd NPs	2.943	[6]
	MXene@AgPd@PDA	1.2	[7]
	Ag–Co/CNF	1.032	[8]
	$Fe_3O_4@AgPd/PDA$	5.95	This work
MO	Ag/ZIF-7	17.28	[9]
	$Fe_3O_4@polythiophen-Ag$	2.82	[10]
	PdNPs/RGO-A	0.6	[11]
	Pd/CCS-Per	1.4	[12]
	$Fe_3O_4@AgPd/PDA$	26	This work
MB	ZBD@Ag	1.83	[13]
	Ag@PDA NTs	3.191	[14]
	$Fe_3O_4@TA/Ag$	2.06	[15]
	12%-Ag/MX/PAM	5.84	[16]
	$Fe_3O_4@AgPd/PDA$	13.35	This work

Table. S3 Heck cross-coupling reactions with different substrates.

Entry	Actant	Product	Conversion (%)	Selectivity (%)
1.			99	>99.8
2.			99.6	>99.9
3.			98.7	>99.9
4.			95.4	>99.9
5.		–	–	–
6.		–	–	–

Reaction conditions: aryl iodide 1 mmol, methyl acrylate 2 mmol, Fe_3O_4@AgPd/PDA catalyst 5 mg, triethylamine (Et_3N) 2 mmol, DMF 5 mL, 100 °C, 5 h.

References

1.   W. Cheng, K. Tang, Y. Qi, J. Sheng and Z. Liu, *Journal of Materials Chemistry*, 2010, **20**, 1799-1805.

2.   A. Feng, Y. Yu, Y. Wang, F. Jiang, Y. Yu, L. Mi and L. Song, *Materials & Design*, 2017, **114**, 161-166.

3.   Q. Xiong, Q. Fang, K. Xu, G. Liu, M. Sang, Y. Xu, L. Hao and S. Xuan, *Dalton Transactions*, 2021, **50**, 14235-14243.

4.   P. A. Bazuła, P. M. Arnal, C. Galeano, B. Zibrowius, W. Schmidt and F. Schüth, *Microporous and Mesoporous Materials*, 2014, **200**, 317-325.

5.   D. Gan, Z. Wang, X. Li, J. Zhou, B. Dai, L. Yang and S. Xia, *Applied Clay Science*, 2023, **244**, 107091.

6.   Z. Kiani, R. Zhiani, S. Khosroyar, A. Motavalizadehkakhky and M. Hosseiny, *Inorganic Chemistry Communications*, 2021, **124**, 108382.

7.   J. Jin, S. Wu, J. Wang, Y. Xu, S. Xuan and Q. Fang, *Dalton Transactions*, 2023, **52**, 2335-2344.

8.   V. K. Landge, S. H. Sonawane, S. Manickam, G. U. Bhaskar Babu and G. Boczkaj, *Journal of Environmental Chemical Engineering*, 2021, **9**, 105719.

9.   A. Malik and M. Nath, *Journal of Environmental Chemical Engineering*, 2020, **8**, 104547.

10.   M. S. Najafinejad, P. Mohammadi, M. Mehdi Afsahi and H. Sheibani, *Journal of Molecular Liquids*, 2018, **262**, 248-254.

11.   M. Hashemi Salehi, M. Yousefi, M. Hekmati and E. Balali, *Applied Organometallic Chemistry*, 2019, **33**.

12.   Z. Farrokhi, S. Sadjadi, F. Raouf and N. Bahri Laleh, *Inorganic Chemistry Communications*, 2022, **143**, 109734.

13.   A. Lajevardi, M. Tavakkoli Yaraki, A. Masjedi, A. Nouri and M. Hossaini Sadr, *Journal of Molecular Liquids*, 2019, **276**, 371-378.

14.   J. Lu, J. Fang, J. Li, C. Wang, Z. He, L. Zhu, Z. Xu and H. Zeng, *ACS Applied Nano Materials*, 2019, **3**, 156-164.

15.   H. Veisi, S. B. Moradi, A. Saljooqi and P. Safarimehr, *Materials Science and*

Engineering: C, 2019, **100**, 445-452.

16.   C. Peng, Z. Kuai, X. Li, S. Lian, D. Jiang, J. Tang, L. Li, R. Wu, A. Wu and S. Chen, *Materials & Design*, 2021, **210**, 110061.